Solubility and Diffusivity of Hydrofluorocarbons in Room-Temperature Ionic Liquids

Mark B. Shiflett [a] ***and A. Yokozeki*** [b]

[a] *DuPont Central Research and Development, Experimental Station E304, Wilmington, DE 19880 U.S.A.E-mail: mark.b.shiflett@usa.dupont.com*

[b] *DuPont Fluoroproducts Laboratory, Chestnut Run Plaza 711, Wilmington, DE 19880 U.S.A. E-mail: akimichi.yokozeki@usa.dupont.com*

Abstract

Gaseous absorption measurements of hydrofluorocarbons (trifluoromethane, difluoromethane, pentafluoroethane, 1,1,1,2-tetrafluoroethane, 1,1,1-trifluoroethane, and 1,1-difluoroethane) in l-*n*-butyl-3-methylimidazolium hexafluorophosphate ([bmim][PF_6]) and 1-*n*-butyl-3-methylimidazolium tetrafluoroborate ([bmim][BF_4]) were performed using a gravimetric microbalance at various isothermal conditions (temperatures between 283.15 and 348.15 K) and at pressures under 2 MPa. This report shows for the first time the solubility and diffusivity data for the hydrofluorocarbons in room-temperature ionic liquids and surprisingly large differences in the solubility among the hydrofluorocarbons. Experimental gas solubility data were successfully correlated with well-known solution models (Margules, Wilson, and NRTL activity coefficient equations). Diffusivities obtained from the time-dependent absorption data were well analyzed using a diffusivity model developed in this study. The calculated molecular size for difluoromethane was 2 to 3 times larger than the known size.

Keywords: ionic liquid, hydrofluorocarbons, solubility, diffusivity, phase equilibria

Introduction

Room-temperature ionic liquids (or, simply called ionic liquids) are molten salts composed of organic cations and inorganic anions. Although they have been known since 1914[1], the research activities on this new type of liquids increased dramatically with the development of the first air-stable and nearly moisture-stable tetrafluoroborate $[BF_4]^-$ ionic liquids in 1992[2]. Now, various ionic liquids are even commercially available since 1999[3].

Due to the extremely large possible combinations of ions, which will be approximately 10^{18} pairs[4], ionic liquids are truly designer solvents. This large number of possible combinations can be used to optimize production costs and thermophysical properties such as solubility, melting points, thermal stability, electric conductivity, thermal conductivity, etc. Another unique feature of ionic

liquids is practically a lack of vapor pressure, hence emissions in engineering applications will be significantly lower than for conventional volatile organic solvents. Therefore, ionic liquids are often called "green solvents" (or environmentally friendly solvents), although sufficient toxicological information is missing at present.

As a new type of solvent, there are numerous possible applications, which will replace the conventional solvents or provide something novel in the application. Whatever the applications will be, fundamental knowledge about thermophysical properties of their mixtures with various chemicals is critically important and needed: for example, solubility of various compounds in ionic liquids with various thermodynamic conditions (*T*, *P*, *x*: temperature, pressure, composition), transport/electric properties such as viscosity, diffusivity, thermal conductivity, electric conductivity, etc. These property measurements as well as theoretical understandings of such properties are largely lacking at present.

In this study, we investigate the solubility and diffusivity of various hydrofluorocarbons (HFCs) in two room-temperature ionic liquids: [bmim][PF_6] and [bmim][BF_4]. HFCs studied here are trifluoromethane (R-23), difluoromethane (R-32), pentafluoroethane (R-125), 1,1,1,2-tetrafluoroethane (R-134a), 1,1,1-trifluoroethane (R-143a), and 1,1-difluoroethane (R-152a). HFCs belong to an important class of compounds in various industrial and household applications. They have been developed as alternative compounds due to the environmental concern of chlorofluorocarbons and hydrochlorofluorocarbons, which were used for refrigerants, blowing agents, propellants, solvents, cleaning agents, fire extinguisher agents, medical applications, etc. The present study is the first systematic investigation of the HFC solubility and diffusivity in ionic liquids; only a couple of works on HFCs in ionic liquids have been so far reported in the literature such as very high pressure solubilities of R-23[5] and electrochemical applications of R-32 or R-134a (no solubility data)[6,7].

The observed solubility data will be analyzed with the conventional solution (activity coefficient) models for non-electrolyte solutions such as Margules, Wilson and nonrandom two-liquid (NRTL) models[8,9], and it will be shown that the non-electrolyte models works very well in the phase equilibrium correlation, even for the ionic-liquid electrolyte solutions. The observed behaviors (diffusivity *versus* *P*, or diffusivity *versus* composition *x*) of the diffusivity data in ionic liquids are successfully explained by a simple semi-theoretical model which has been developed in this study. The solubility and diffusivity of CO_2 / ionic-liquid solutions in our previous study[10] are also compared with the present HFC results.

Experimental Procedures and Results

Materials and experiment

The [bmim][PF_6] (Lot and Filling code, 1055432 31304010) and [bmim][BF_4] (Lot and Filling Code, 1080045 11304079) were obtained from Fluka

Chemika with a purity of >96 and >97%, respectively. The chloride content was measured by ion chromatography, and the extractable chloride content as purchased for [bmim][PF_6] and [bmim][BF_4] was 4.7 and 1.6 g m^{-3}, respectively. R-23, R-32, R-125, R-134a, R-143a, and R-152a were obtained from DuPont Fluoroproducts with a minimum purity of 99.9%. A molecular sieve trap was installed to remove trace amounts of water from the gases. Special care was taken to use separate molecular sieve traps for each gas in order to prevent cross-contamination.

The gas solubility and diffusivity measurements were made using a gravimetric microbalance (Hiden Isochema Ltd, IGA 003) as described in our previous report[10]. Initially, 60 to 80 mg of ionic liquid was loaded into the sample container and heated to 348.2 K under a vacuum of about 10^{-9} MPa for 10 hr to remove any trace amounts of water or other impurities. Four isotherms were measured at 283.2 (or 285.2), 298.2, 323.2, and 348.2 K over a pressure range from about 0.01 to 2.0 MPa. The upper pressure limit for each gas was dependent on the saturation pressure in the sample container at ambient temperature. To ensure sufficient time for gas-liquid equilibrium, the ionic liquid samples were maintained at each pressure set-point for a minimum of 3 hr with a maximum time-out of 10 hr.

Error analysis

The instrumental uncertainties in *T* and *P* are within 0.1 K and 0.8 kPa, respectively. These errors do not cause any significant changes in the gas solubility (mole fraction) measurement. One of the largest error sources in the present experiment is data reproducibility. We have examined the data reproducibility by repeating the experiments in different times (for example, one month apart for the same binary system). Our best estimate for the present experimental reproducibility error, including the sample (ionic liquid) purity effect, has been less than 0.005 mole fraction. The next largest systematic error is due to the buoyancy correction in the data analysis.

When gas dissolves in ionic liquid, the liquid volume will change. The change in liquid volume affects the buoyancy force in the gravimetric microbalance. Here we estimate a systematic error (or the correction term) in solubility (mole fraction) due to neglecting the volume change of a gas-dissolved ionic liquid. A volume (V_L) of gas-dissolved liquid may safely be assumed to be a mole fraction average of molar volumes of each constituent species, since we are interested in only a minor correction term:

$$V_L = \tilde{V}_1 \frac{w_1}{M_1} + \tilde{V}_0 \frac{w_0}{M_0}, \qquad (1)$$

where subscripts 1 and 0 mean a sample gas and an ionic liquid, respectively, and

w = amount of weight in the liquid mixture,
M = molar mass,

$\widetilde{V}$ = molar saturated-liquid volume at a given *T*.

A liquid volume change, δV_L , due to the gas absorption amount, δw_1, is:

$$\delta V_L = \frac{\widetilde{V}_1}{M_1}\delta w_1 . \quad (2)$$

Then, the actual weight reading (w_1) in the microbalance must be corrected by adding the buoyancy effect (a small amount of weight, δw_1) due to δV_L:

$$\delta w_1 = \frac{\widetilde{V}_1}{M_1}\delta w_1 \rho_g(T,P) = \widetilde{V}_1 \delta w_1 \widetilde{\rho}_g , \quad (3)$$

where $\rho_g(T,P)$ is a super-heated gas density at the system *T* and *P*, and $\widetilde{\rho}_g$ is the corresponding molar density, which can be calculated as well as $\widetilde{V}_1$ by a REFPROP computer code[11]. After some algebraic manipulations, Eq. 3 can be converted to a molar correction term, δx_1:

$$\delta x_1 = x_1(1-x_1)\widetilde{\rho}_g \widetilde{V}_1 . \quad (4)$$

For example, using actual experimental data of x_1 = 0.8121 (uncorrected mole fraction) for a (1)R-32 / (2)[bmim][PF_6] system at 283.2 K and 0.8495 MPa, Eq. 4 gives the correction term of 0.0033 mole fraction, where $\widetilde{\rho}_g = 0.0004194$ mol cm^{-3} and $\widetilde{V}_1 = 51.021$ cm^{-3} mol from REFPROP[11].

Thus, the systematic error due to the volume change in the liquid solution can be corrected with Eq. 4, as long as $\widetilde{\rho}_g$ and $\widetilde{V}_1$ are known. Unfortunately, $\widetilde{V}_1$ is only calculated for temperatures below T_c (critical temperature of gaseous species 1) with REFPROP[11] (or any equations of state). Since some of our experimental conditions exceed T_c, a proper method to estimate $\widetilde{V}_1$ in all temperatures including those above T_c has to be developed. Here, we propose the following simple equation of $\widetilde{V}_1$ for all temperatures:

$$\widetilde{V}_1 = (1-\alpha_v)\widetilde{V}_0 , \quad (5)$$

where $\widetilde{V}_0$ is a molar liquid volume of ionic liquid at *T* and α_v is a unique temperature-independent constant for each binary system, described below.

For [bmim][PF_6], $\widetilde{V}_0$ is given by:

$$\widetilde{V}_0[\mathrm{cm}^3/\mathrm{mol}] = \frac{M_0}{\rho_L} = \frac{284.18}{1.619874 - 8.441224\times10^{-4}T[K]} , \quad (6)$$

and for [bmim][BF_4]:

$$\widetilde{V}_0[\mathrm{cm}^3/\mathrm{mol}] = \frac{M_0}{\rho_L} = \frac{226.02}{1.412932 - 7.056735\times10^{-4}T[K]} . \quad (7)$$

Coefficients in ρ_L (liquid density of ionic liquid) were obtained by fitting experimental liquid densities of ionic liquids[10]. Equation 5 is based on our

previous report[10], where we have found a molar liquid volume of a mixture, $\widetilde{V}_m$, can be well correlated with the following simple equation:

$$\frac{\Delta\widetilde{V}}{\widetilde{V}_0} \equiv \frac{\widetilde{V}_m}{\widetilde{V}_0} - 1 \approx -\alpha_v x_1, \tag{8}$$

where α_v (> 0) is nearly independent of temperatures (even for those above T_c). Then, if we assume $\widetilde{V}_m$ is equal to a mole fraction average of each constituent molar volume, Eq. 5 can be derived. Estimated values in α_v from the slope in the plot of Eq. 8 range from 0.5 to 0.75.

Although Eq. 5 is a rough estimate, it is sufficient for the present purpose, since we are dealing here with a minor correction term using Eq. 4. We have estimated a systematic error due to the use of the approximation Eq. 5 to be less than 0.002 mole fraction, comparing the results with the use of the accurate $\widetilde{V}_1$ (below T_c of REFPROP[11]). Thus, total errors in the solubility data due to both random and systematic errors have been estimated to be less than 0.006 mole fractions at given *T* and *P*.

Concerning errors in the diffusivity data, the largest error source comes from experimental reproducibility (random) errors. They were estimated to be roughly within a factor of two in the determined diffusivity, based on the scatters of various analyzed diffusivity data. The second largest error source in the diffusivity data is due to the assumed liquid-depth parameter, *L* (see the following section for the diffusivity result) in the analysis, which was assumed to be constant. However, *L* varies with the amount of gas absorption, due to the liquid expansion by the gas absorption. Errors by this variable *L* in the analysis showed less than about 60 % effect in the final diffusivity data. Thus, the overall error limit in the diffusivity of a factor of two, cited above, will cover this systematic error as well.

Results

Figure 1 shows a plot of normalized-pressures (or more precisely, normalized-fugacities at 298.2 K) *vs*. molar compositions, which measures the deviation from the ideal solubility behavior (Raoult's law). Surprisingly large differences in the solubility among the same family of compounds (hydrofluorocarbons) are clearly observed: e.g., from a slightly negative deviation in R-32 to a highly positive deviation in R-143a. These behaviors are quite unexpected.

Although Henry's law constants do not tell the whole story about actual solubility behaviors of gases, they are often reported in literature as the limiting solubility at the infinite dilution. The Henry's law constant (*H*) is defined as:

$$H = \lim_{x \to 0} \frac{f(T, P, y)}{x}, \tag{9}$$

f: vapor-phase fugacity of solute (vapor composition, *y*) at the system *T* and *P*,

x: liquid-phase solute mole fraction,
y: vapor-phase solute mole fraction.

In the present case, $f(T,P,y)$ can be treated as the pure vapor fugacity of the solute species (*y* = 1), due to the negligible vapor pressure of ionic liquids. However, Eq. 9 has a problem, since it becomes indeterminate (*i.e.*, approaches 0/0) at the limit (*x* = 0). This problem can be resolved by the use of l'Hôpital's rule, which gives,

$$H \approx \left(\frac{df}{dx}\right)_{x=0}, \tag{10}$$

where *f* is an empirically fitted fugacity as a function of *x* at each isotherm; here we have used a second-order polynomial function for *f*.

Diffusivity (*D*) was obtained from the analysis of time-dependent absorption data, < *C* >, using the following model equation[10,12]:

$$< C >= C_S\left[1-2\left(1-\frac{C_0}{C_S}\right)\sum_{n=0}^{\infty}\frac{\exp\left(-\lambda_n^2 D t\right)}{L^2\lambda_n^2}\right], \tag{11}$$

where $\lambda_n=\left(n+\frac{1}{2}\right)\frac{\pi}{L}$, C_0 and C_S are the initial and final concentrations of a solution mixture, respectively, and *L* is the liquid depth of the solution in a test container. Detail procedures of the analysis are given in Ref. 10.

Data Correlation

In this section, we first analyze the experimental solubility (*T*, *P*, *x*) data with the existing solution models for non-electrolyte solutions, which may also be applied even for electrolyte solutions, particularly for the case of the phase-boundary correlation (e.g., vapor liquid equilibria)[13-16]. In fact, all observed solubility behaviors in the present ionic solutions have been well correlated using the well-known solubility models for non-electrolyte solutions. Next, in the diffusivity model subsection, we develop a semi-theoretical model for diffusivity data of general solutions and apply it successfully to the present diffusivity data.

Solubility model

In general, low-and-medium pressure VLE (vapor liquid equilibria) for an *N*-component system can be described by[17]:

$$y_i P\Phi_i = x_i \gamma_i P_i^s, \quad (i = 1, .., N), \tag{12}$$

where

y = vapor phase mole fraction,
x = liquid phase mole fraction,

P = system pressure,
P_i^s = saturated vapor pressure of *i-th* species,
γ = activity coefficient (function of compositions and T),
Φ_i = a correction factor for *i-th* species ($\approx$ 1 for sufficiently low P systems).

For a binary system (N = 2) of gas (1) / ionic liquid (2) mixtures, it is reasonable to assume that y_1 = 1 (or y_2 = 0) at temperatures of the present interest; *i.e.*, $P_2^s \approx 0$. Then, the activity coefficient for species 1 is given by Eq. 12:

$$\gamma_1 = \frac{P\Phi_1}{x_1 P_1^s}. \tag{13}$$

The correction factor Φ_1 is for the present case[17]:

$$\Phi_1 = \exp\left[\frac{\left(B_1 - \tilde{V}_1\right)\left(P - P_1^s\right)}{RT}\right], \tag{14}$$

where

B_1 = 2nd virial coefficient of species 1 at system T,
$\tilde{V}_1$ = saturated molar liquid volume of species 1 at system T,
R = universal gas constant.

$B_1(T)$ can be obtained, for example, from Ref. 18 or by a REFPROP computer code[11] and similarly $\tilde{V}_1$ can be calculated if T is less than the critical point T_c of a pure component 1. In the present analysis, however, we adopt an approximate $\tilde{V}_1$, which is defined earlier by Eq. 5, and can be applied even for temperatures above T_c. It should be mentioned here that the present approximate $\tilde{V}_1$ in Eq. 5 is sufficient for the present data analysis with Eqs. 12-14, since it is used merely in the correction term, Φ_1.

Concerning the vapor pressure of pure species 1, we use an Antoine type equation for temperature variations:

$$\ln P_1^s = A_1 - \frac{B_1}{T + C_1}. \tag{15}$$

Coefficients in Eq. 15 were determined by fitting P_1^s (from REFPROP[11]) between 283.2 and 348.2 K (or T_c), and we assume that Eq. 15 holds even above T_c as an extrapolated hypothetical vapor pressure.

Now, we are ready to analyze experimental solubility data using the activity coefficient of Eq. 13. For each isothermal solubility data, the activity coefficients γ_1 were calculated at each observed x_1 point. Several activity models are available in the literature[8,9]. In this work, we examined three commonly used models: the two-parameter Margules, Wilson, and NRTL equations. The activity coefficients by the Margules model are:

$$\ln \gamma_1 = \left[A + 2(B - A)x_1\right]x_2^2, \tag{16}$$

$$\ln \gamma_2 = \left[B + 2(A - B)x_2\right]x_1^2. \tag{17}$$

A, *B*: adjustable binary interaction parameters. (18)

In the case of the Wilson model:

$$\ln \gamma_1 = -\ln\left(x_1 + \Lambda_{12}x_2\right) + x_2\left(\frac{\Lambda_{12}}{x_1 + \Lambda_{12}x_2} - \frac{\Lambda_{21}}{\Lambda_{21}x_1 + x_2}\right), \tag{19}$$

$$\ln \gamma_2 = -\ln\left(x_2 + \Lambda_{21}x_1\right) - x_1\left(\frac{\Lambda_{12}}{x_1 + \Lambda_{12}x_2} - \frac{\Lambda_{21}}{\Lambda_{21}x_1 + x_2}\right), \tag{20}$$

where

$$\Lambda_{12} \equiv \frac{V_2^L}{V_1^L}\exp\left(-\lambda_{12}\right), \text{ and } \Lambda_{21} \equiv \frac{V_1^L}{V_2^L}\exp\left(-\lambda_{21}\right), \tag{21}$$

$\lambda_{12} \equiv \frac{\Delta\lambda_1}{RT}$, and $\lambda_{21} \equiv \frac{\Delta\lambda_2}{RT}$: (adjustable binary interaction parameters), (22)

V_i^L: molar volume of pure liquid component *i*.

In the case of the NRTL model:

$$\ln \gamma_1 = x_2^2\left[\tau_{21}\left(\frac{G_{21}}{x_1 + x_2G_{21}}\right)^2 + \frac{\tau_{12}G_{12}}{\left(x_2 + x_1G_{12}\right)^2}\right], \tag{23}$$

$$\ln \gamma_2 = x_1^2\left[\tau_{12}\left(\frac{G_{12}}{x_2 + x_1G_{12}}\right)^2 + \frac{\tau_{21}G_{21}}{\left(x_1 + x_2G_{21}\right)^2}\right], \tag{24}$$

where

$$G_{12} \equiv \exp\left(-\alpha\tau_{12}\right), \text{ and } G_{21} \equiv \exp\left(-\alpha\tau_{21}\right), \tag{25}$$

$\tau_{12} \equiv \frac{\Delta g_1}{RT}$, and $\tau_{21} \equiv \frac{\Delta g_2}{RT}$: (adjustable binary interaction parameters). (26)

$\alpha = 0.2$ (assumed to be a constant of 0.2 in this work).

The temperature-dependent binary interaction parameter (p_{ij}) is often modeled by[8,16]:

$$p_{ij} = p_{ij}^{(0)} + p_{ij}^{(1)}/T + p_{ij}^{(2)}T. \tag{27}$$

In this study, we have modeled all p_{ij} by the first two terms for Eqs. 18, 22, and 26:

$$A = A^{(0)} + A^{(1)}/T, \text{ and } B = B^{(0)} + B^{(1)}/T, \tag{28}$$

$$\lambda_{12} = \lambda_{12}^{(0)} + \lambda_{12}^{(1)}/T, \text{ and } \lambda_{21} = \lambda_{21}^{(0)} + \lambda_{21}^{(1)}/T, \tag{29}$$

$$\tau_{12} = \tau_{12}^{(0)} + \tau_{12}^{(1)}/T, \text{ and } \tau_{21} = \tau_{21}^{(0)} + \tau_{21}^{(1)}/T. \tag{30}$$

The adjustable parameters in Eqs. 28-30 can be obtained by fitting Eq. 13 with the activity coefficient models of Eq. 16 (Margules), Eq. 19 (Wilson), or Eq. 23 (NRTL).

Another method to obtain the binary interaction parameters is to fit directly the experimental pressure data. The calculation of pressures at a given *T* can be made using Eqs. 13 and 14 with the proper activity coefficient model (Eq. 16, 19, or 23), but *P* is not a pressure-explicit form. This requires iterative calculations; a Newton-Raphson method works very well here. From Eqs. 13 and 14, the implicit pressure equation is:

$$\ln P + \left(P - P_1^s\right)\left(B_1 - \widetilde{V}_1\right)/RT - \ln P_1^s - \ln\left(x_1\gamma_1\right) = 0\,, \qquad (31)$$

where P_1^s is given by Eq. 15, $\widetilde{V}_1$ is given by Eq. 5, γ_1 is calculated by Eq. 16, 19, or 23, and B_1 can be obtained from Ref. 18, or a REPPROP program[11].

We have analyzed the experimental solubility data using both methods (Eqs. 13 and 31), and found that both analyses give equivalent results. Therefore, in this report, we only show the results with the pressure fitting method (using Eq. 31). In addition, the three activity-coefficient models (Margules, Wilson, and NRTL) provided equally good data correlation. Figure 2 shows an example for the comparison of isothermal *Px* plots using the R-134a/[bmim][PF_6] system. The binary interaction parameters used in Figure 2 are $A^{(0)}$ = 2.512, $A^{(1)}$ = -541.47 K, $B^{(0)}$ = 0.2439, and $B^{(1)}$ =357.10 K in Eq. 28, $\lambda_{12}^{(0)}$ = 1.6894, $\lambda_{12}^{(1)}$ = -261.25 K, $\lambda_{21}^{(0)}$ = 0.8232, and $\lambda_{21}^{(1)}$ = 138.46 K in Eq. 29, and $\tau_{12}^{(0)}$ = -3.001, $\tau_{12}^{(1)}$ = 1699.2 K, $\tau_{21}^{(0)}$ = 2.5102, and $\tau_{21}^{(1)}$ = -1000.0 K in Eq. 30, respectively. Standard deviations in the pressure fit are 0.004, 0.005 and 0.004 MPa for the Margules, Wilson, and NRTL models, respectively. As far as the VLE correlation is concerned, the three models were equally acceptable for all binary systems studied here. However, the Margules equation is a good model but purely empirical (i.e., simply empirical polynomials), while both Wilson and NRTL activity coefficients have some theoretical foundations but the Wilson model is only applicable for VLE (*i.e.*, no LLE prediction)[8]. In this article, we report the results of the solubility correlation only with the NRTL model.

Determined binary interaction parameters in Eq. 30 are listed in Table 1 for the present binary systems as well as our previous CO_2/ionic liquids[10]. Isothermal *Px* diagrams calculated with these parameters are compared with observed values and an example for R-134a in [bmim][PF_6] is provided in Figure 3.

Diffusivity model

A diffusion coefficient, D_{AB}, of a dilute solute A (spherical body with a radius r_A) in a solvent B (viscosity η_B), is given by the Einstein-Stokes equation[9,19]:

$$D_{AB} = \frac{kT}{6\pi r_A \eta_B}. \quad (32)$$

k: Boltzmann constant; *T*: temperature.

This equation may be a starting point in developing empirical correlations for diffusivity data in general liquid solutions. In addition, it is well known empirically that the mutual diffusion coefficient, *D*, in liquid is correlated with the solution viscosity, η; $D \propto \eta^{-n}$, where usually $0.5 \le n \le 1$ for various compounds[9]. Then, we propose the following empirical form as a modified Einstein-Stokes equation:

$$D = \frac{kT}{6\pi r \eta_0 (\eta/\eta_0)^b}, \quad (33)$$

or

$$\ln(D/T) = a - b\ln(\eta/\eta_0), \quad (34)$$

where $a = \ln(k/6\pi r\eta_0)$ and η_0 is a unit viscosity (e.g., 0.001 Pa·s in the SI unit); this unit viscosity is needed as a normalization factor for the equation to have the proper dimension. When *b* = 1 and $a = \ln[k/6\pi r_A]$, Eq. 33 becomes Eq. 32. Thus, the proposed equation can be regarded as a generalized Einstein-Stokes equation for a general solution with adjustable parameters *a* and *b*. Concerning the solution viscosity in Eq. 34, we adopt our earlier model for an *N*-component solution viscosity[20]:

$$\ln(\eta/\eta_0) = \sum_{i=1}^{N} \xi_i \ln(\eta_i/\eta_0), \quad (35)$$

where

$$\xi_i = m_i^c x_i \Big/ \sum_{i=1}^{N} m_i^c x_i, \quad (36)$$

m_i: molecular weight of *i-th* species; x_i: mole fraction of *i-th* species;

η_i: dynamic viscosity of *i-th* species; *c*: adjustable parameter;

η_0: unit viscosity in order to make the equation dimensionless.

It is instructive to note that if *c* = 1, Eq. 36 means a mass fraction, while if *c* = 0, then it is simply a mole fraction. The usefulness of Eq. 35 has been stated in Ref. 21. The present diffusivity model, Eq. 34 with Eq. 35, has three empirical adjustable parameters (*a*, *b*, and *c*) to correlate observed diffusivity data (function of *x*, and *T*), provided that the viscosity of each pure species is known. The absolute viscosity of a pure compound *i* is modeled as:

$$\ln\eta_i = A_i + \frac{B_i}{T} + C_i T + D_i T^2. \quad (37)$$

The adjustable parameter *c* is nonlinear in Eqs. 34 and 35, and we have found it is a rather insensitive parameter to the correlation with values between 0 and 1. Thus, instead of using a nonlinear regression analysis, we used several

fixed trial values in *c* between 0 and 1, and then applied a linear regression analysis of Eq. 34 to obtain the parameters *a* and *b*. Determined parameters for several systems are listed in Table 2, and model calculations with these parameters are compared with experimental diffusivity data where the pressure axis was calculated by the *Px* diagram of the NRTL correlation. Figure 4 shows an example of *D versus x* plots using a case of the R-152a / [bmim][PF_6] system. All *D versus x* plots are qualitatively similar; *D* increases with *x* monotonically without crossing each other. The model calculation is generally in good agreement with the experimental data (within about a factor of two), which are often scattered with rather large uncertainties.

It is interesting to see that the *b* parameters in Table 2 for ionic liquid solutions have magnitudes similar to those known in various non-electrolyte solutions[9]: between 0.5 and 1.0. The empirical *a* parameter in Eq. 34 can possess a physical meaning: $a = \ln(k/6\pi r\eta_0)$. If the present model with Eq. 33 or 34 is physically meaningful, the determined *a* parameters should provide reasonable values in *r* (effective molecular radius of solute), or at least a physically correct order of magnitude. Values from –25.7 to –27.5 in *a* (see Table 2) give *r* = 0.10 to 0.61 nm, which are indeed physically reasonable values, compared with molecular diameters (0.33 to 0.46 nm) of HFCs (R-23, R-32, R-125, R-134a, R-143a, and R-152a)[18] and CO_2 (about 0.2 nm)[19]. It is expected that the molecular size of CO_2 will be the smallest among the systems studied here. Indeed, *r* values in CO_2 are the smallest: *r* (in [bmim][PF_6]) = 0.10 nm and *r* (in [bmim][BF_4]) = 0.15 nm. These values are reasonable compared with a reported molecular radius of CO_2, which is about 0.20 to 0.23 nm, based on the molecular diameter of CO_2[19].

Discussion

In this report, we have discovered large differences in the solubility among HFCs in an ionic liquid, [bmim][PF_6]. Similar solubility behaviors will be expected for HFCs in other ionic liquids such as [bmim][BF_4], some of which have been studied in this work. At first glance, these solubility differences are surprising, by considering the fact that the same type of compounds usually show similar VLE (solubility) behaviors in a given type of solvent. HFC compounds are known to possess large electric dipole moments (or, highly polar compounds), and ionic liquids, which may be also regarded as highly polar solvents, are likely to explain the observed solubility behavior. However, the magnitude of the electric dipole moment of HFCs does not correlate the observed solubility trend. The dipole moments of R-152a, R-143a, R-134a, R-125, R-32 and R-23 are 2.262, 2.340, 2.058, 1.563, 1.978, and 1.649 debye, respectively[11,18], while R-32 is most soluble and R-143a is least soluble; or the solubility order in solvent-rich side solutions is R-32 > R-152a > R-23 > R-134a > R-125 > R-143a (see Figure 1).

Another unique property in HFCs is their H-bonding capability (H -- F -- H), but their role in the present solubility behavior is not obvious. It is also interesting

to observe that CO_2 has also fairly high solubility at least in [bmim][PF_6]-rich side solutions, as shown in Figure 1. CO_2 is non-polar (no electric dipole moment), although it possesses a relatively large quadrupole moment[22], and has π electrons (conjugated double bonds). Charge-transfer complex formations, solvations of ions, molecular associations, etc. may be involved, but at present no specific or integrated intermolecular forces are identified as being responsible for the observed solubility behavior.

Although we don't have a clear understanding on a molecular level, the present solubility difference can be used for engineering processes such as extractive distillations or extraction solvents[16]. Both binary mixtures of R-32 / R-125 and R-125 / R-143a are azeotropic systems and important refrigerants. Purification or reuse of these refrigerants as recovery products will be particularly suited with the present ionic liquids, because of the significantly large solubility differences.

All solubility (VLE) data of the present binary systems with ionic liquids have been successfully correlated with the conventional activity models for non-electrolyte solutions. However, the present results are not surprising, since several successful attempts using non-electrolyte models for electrolyte solutions have been known in the literature [13-16]. Treating the ionic liquid as an undissociated species may not be a bad assumption in the present case. Most of the electrolyte-solution models assume the complete dissociation, which is, however, not always a correct assumption. As far as the phase behavior correlation is concerned, it seems well known that non-electrolyte-solution models work well even for electrolyte solutions[15].

The prediction of LLE (liquid-liquid equilibria) based on only VLE data, or vice versa, is not numerically accurate in the conventional activity models[8]. However, it is interesting to show that the present NRTL model analyses predict LLE for the case of ionic liquid mixtures with R-143a, see Figure 5. The predicted phase behaviors will be correct at least qualitatively, and it is also predicted that the immiscibility gap (of LLE) decreases as T decreases, indicating that it has a LCST (lower critical solution temperature). A similar phase behavior has been predicted in our previous report on CO_2 /ionic liquid systems[10]. However, it should be mentioned here that the present activity models (or any solution models), Eq. 12, is inaccurate (or undefined) at high temperatures, particularly near and above T_c of gaseous species. Thus, extrapolations for phase behaviors over wide temperature ranges must be treated with a great caution. More reliable predictions of large-scale (global) phase behaviors may be made using proper equations of state, which will be reported in a separate paper[23], where we will show that binary HFC and CO_2 systems with the present ionic liquids belong to the Type-V fluid, according to the classification of Scott and van Konynenburg [22,26,27].

Finally, it is quite pleasing to see that the observed diffusivity behaviors (in *D vs*. *P*, or *D vs*. *x* plots) have been well explained by a simple diffusion model, developed in the present study. The model is based on the theoretical Stokes-Einstein model plus a well-known empirical relation between solution viscosity and diffusivity[9], and the solution viscosity model is taken from our previous work[20]. As discussed in the diffusivity modeling section, the empirical fitting parameter, *a* in Eq. 34, may contain a physically meaningful quantity: *i*.*e*., the size of the diffusing body. In fact, in the case of CO_2 in the ionic liquids, the present model (*a*) provided a molecular size that is close to the known CO_2 molecular size[19]. Then, a question is what about other systems. If we take the present model parameter, *a*, numerically seriously, based on the results of CO_2, the size of diffusing bodies of HFCs in the ionic liquids are also similar to the typical molecular size of HFCs.[18] However, among all HFCs studied here, R-32 has the smallest molecular size and the derived diffusing body size is the largest: 2 (in [bmim][BF_4]) to 3 (in [bmim][PF_6]) times larger than the known size of R-32.[18] It is intriguing to imagine that among the HFCs studied, R-32 diffuses in the ionic liquids as clusters (or molecular associations). Some spectroscopic experiments might prove such behaviors.

Conclusions

We have published the solubility and diffusivity of an important class of compounds, hydrofluorocarbons (HFCs), in commonly known ionic liquids: [bmim][PF_6] and [bmim][BF_4].[28] To our best knowledge, these studies have not been reported in the literature. We have found amazingly different solubilities among HFCs in the ionic liquids. Although the mechanism of the solubility difference is not clear in an intermolecular level, the engineering applications due to the present discovery are quite significant in the field of material separations among HFCs, such as extractive distillation, extraction solvents, etc. The observed VLE (*P, T, x*) behaviors of electrolyte (ionic liquid) solutions with HFCs have been well correlated with the conventional solution (activity coefficient) models for non-electrolyte solutions. Diffusivity data of HFCs in the ionic liquids are obtained for the first time in this work. The observed behaviors of the isothermal diffusivity in the pressure or composition space have been successfully correlated with a model developed in this study.

Literature Cited

1. Walden P. Molecular weights and electrical conductivity of several fused salts. *Bull. Acad. Imper. Sci*. St. Petersburg 1914;405:22.
2. Wilkes JS, Zaworotko MJ. Air and water stable 1-ethyl-3-methylimidazolium based ionic liquids. *J. Chem. Soc. Chem. Commun*. 1992;965.
3. Solvent Innovation. 2005; http://www.solvent-innovation.com.
4. Holbrey JD, Seddon KR. Ionic liquids. *Clean Products and Processes* 1999;1:223-236.
5. Shariati A, Peters CJ. High-pressure phase behavior of systems with ionic liquids: measurements and modeling of the binary system fluoroform + 1-

ethyl-3-methylimidazolium hexafluorophosphate. *J. Supercrit. Fluids* 2003;25:109-117.
6. Abbott AP, Eardley CA, Harper CJ, Hope GE. Electrochemical investigations in liquid and supercritical 1,1,1,2-tetrafluroroethane (HFC 134a) and difluoromethane (HFC 32). *J. Electroanal. Chem*. 1998;457:1-4.
7. Abbott AP, Eardley CA. Conductivity of $(C_4H_9)_4N$ BF_4 in liquid and supercritical hydrofluorocarbons. *J. Phys. Chem. B*. 2000;104:9351-9355.
8. Walas SM. *Phase equilibria in chemical engineering*. Boston: Butterworth, 1985;178-183.
9. Reid RC, Prausnitz JM, Poling BE. *The properties of gases and liquids*. 4th ed. New York: McGraw-Hill, 1987.
10. Shiflett MB, Yokozeki A. Solubilities and diffusivities of carbon dioxide in ionic liquid: [bmim][PF_6] and [bmim][BF_4]. *Ind. Eng. Chem. Res*. 2005;44:4453-4464.
11. Lemmon EW, McLinden MO, Huber ML. A computer program, REFPROP (ver. 7). National Institute of Standards and Technology, Gaithersburg, MD 2002.
12. Yokozeki A. Time-dependent behavior of gas absorption in lubricant oil. *Int. J. Refrigeration* 2002;22:695-704.
13. Kato R, Krummen M, Gmehling J. Measurement and correlation of vapor-liquid equilibria and excess enthalpies of binary sytems containing ionic liquids and hydrocarbons. *Fluid Phase Equilibr.* 2004;224:47-54.
14. Döker M, Gmehling J. Measurement and prediction of vapor-liquid equilibria of ternary systems containing ionic liquids. *Fluid Phase Equilibr*. 2005;227:255-266.
15. Anderko A, Wang P, Rafal, M. Electrolyte solutions: from thermodynamic and transport property models to simulation of industrial processes. *Fluid Phase Equilibr*. 2002;194-197:123-142.
16. Seiler M, Jork C, Kavarou A, Arlt W, Hirsch R. Separation of azeotropic mixtures using hyperbranched polymers or ionic liquids. *AIChE J*. 2004;50:2439-2454.
17. Van Ness CH, Abbott MM. *Classical Thermodynamics of Nonelectrolyte Solutions*. New York: McGraw-Hill, 1982.
18. Yokozeki A, Sato H, Watanabe K. Ideal-gas heat capacities and virial coefficients of HFC refrigerants. *Int. J. Thermophys*. 1998;19(1):89-127.
19. Hirschfelder JO, Curtiss CF, Bird RB. *Molecular theory of gases and liquids*. New York: John Wiley, 1964;1111.
20. Yokozeki A. Solubility and viscosity of refrigerant-oil mixtures. *Proc. Int. Compr. Eng. Conference*. Purdue Univ. West Lafayette, Indiana. 1994;1:335-340.
21. Michels HH, Sienel TH. *Proc. of Int. Conf. Ozone Protection Tech*. Baltimore, MD 1997;96-105.
22. Rowlinson JS, Swinton FL. *Liquids and Liquid Mixtures*. 3rd ed. London: Butterworth, 1982.
23. Yokozeki A, Shiflett MB. Global phase behaviors of hydrofluorocarbons in ionic liquids. 2005; (to be published).

24. Geller V, Paulaitis M, Bivens D, Yokozeki A. Transport properties and heat transfer of alternatives for R502 and R22. *Proc. ASHRAE / NIST Refrigerants Conf*., ASHRAE 1996:73-78.
25. Thermophysical Properties of Environmentally Acceptable Fluorocarbons: HFC-134a and HCFC-123. *Japanese Assoc. Refrigeration*, Tokyo 1990:61.
26. Scott RL, van Knoynenburg PH. Static properties of solutions. Van der Waals and related models for hydrocarbon mixtures. *Discuss. Faraday Soc*. 1970;49:87-97.
27. van Knoynenburg PH, Scott RL. Critical lines and phase equilibria in binary van der Waals mixtures. *Philos. Trans*. 1980;A298:495-540.
28. Shiflett MB, Yokozeki A. Solubility and Diffusivity of Hydrofluorocarbons in Room-Temperature Ionic Liquids. *AIChE J*. **2005** (in press).

Table 1. Determined Parameters of Eq. 30 for the NRTL Activity-Coefficient Model.

System (1)/(2)	$\tau_{12}^{(0)}$	$\tau_{12}^{(1)}$ [K]	$\tau_{21}^{(0)}$	$\tau_{21}^{(1)}$ [K]	δP [MPa]*
CO_2/[bmim][PF_6]	-4.663	2806.8	1.0656	-812.37	0.0078
CO_2/[bmim][BF_4]	-2.454	2209.6	0.8119	-723.52	0.0076
R-23/[bmim][PF_6]	4.303	-313.31	-0.1424	-353.02	0.0168
R-32/[bmim][PF_6]	4.408	-565.89	-1.0275	-199.06	0.0067
R-32/[bmim][BF_4]	0.6154	714.11	0.5525	-674.40	0.0078
R-125/[bmim][PF_6]	2.788	-78.28	1.2041	-422.79	0.0084
R-134a/[bmim][PF_6]	-3.001	1699.2	2.5102	-1000.0	0.0043
R-143a/[bmim][PF_6]	6.266	-251.81	-0.1725	-53.31	0.0043
R-152a/[bmim][PF_6]	-2.506	1834.4	1.9383	-1000.0	0.0058

*Standard deviations in pressure of the non-linear regression analysis with α = 0.2: see text.

Table 2. Determined Parameters in Eqs. 34 and 36.

System	*a*	*b*	*c*	*r (nm)*
CO_2/[bmim][PF_6]	-25.660 ± 0.104	0.664 ± 0.020	0.7	0.10
CO_2/[bmim][BF_4]	-26.033 ± 0.139	0.644 ± 0.034	0.7	0.15
R-23/[bmim][PF_6]	-26.581 ± 0.160	0.603 ± 0.034	0.5	0.26
R-32/[bmim][PF_6]	-27.452 ± 0.106	0.474 ± 0.026	0.5	0.61
R-32/[bmim][BF_4]	-27.229 ± 0.109	0.560 ± 0.032	0.5	0.49
R-125/[bmim][PF_6]	-26.412 ± 0.148	0.727 ± 0.032	0.5	0.22
R-134a/[bmim][PF_6]	-26.420 ± 0.171	0.714 ± 0.037	0.5	0.22
R-143a/[bmim][PF_6]	-26.054 ± 0.210	0.793 ± 0.043	0.5	0.15
R-152a/[bmim][PF_6]	-26.052 ± 0.142	0.748 ± 0.031	0.5	0.15

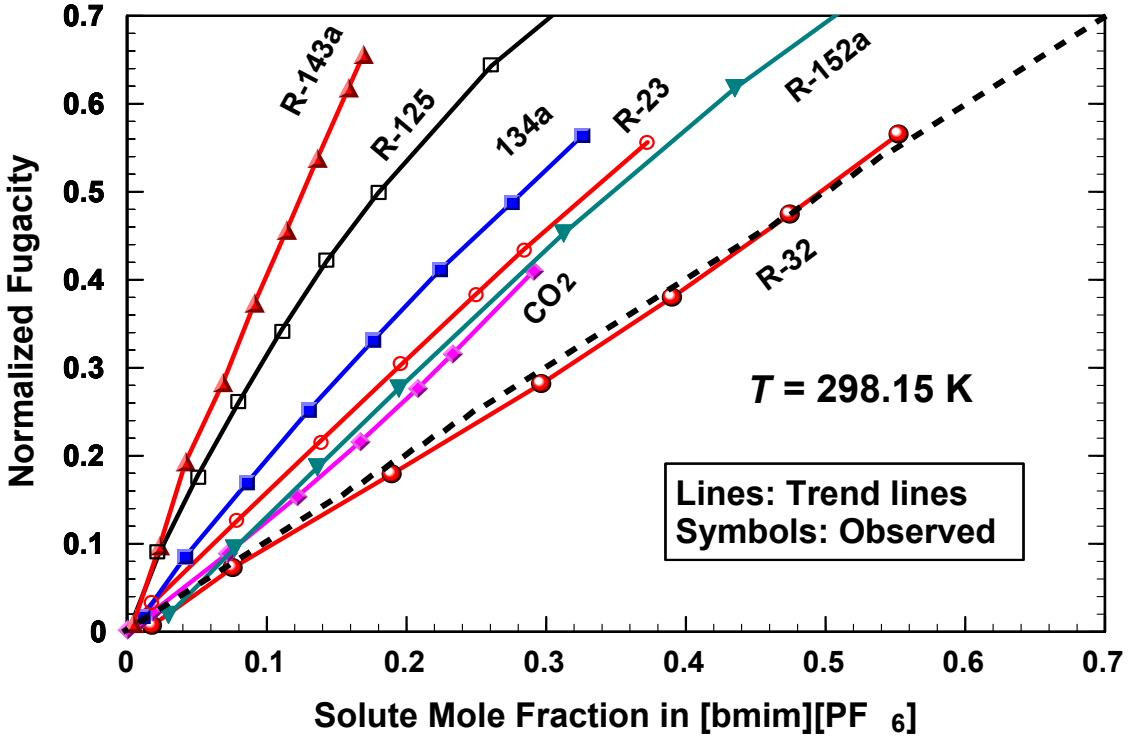

Figure 1. Normalized fugacities *versus* compositions at 298.2 K. The fugacity is normalized by that in the saturated liquid of the pure solute. The dashed line represents Raoult's law.

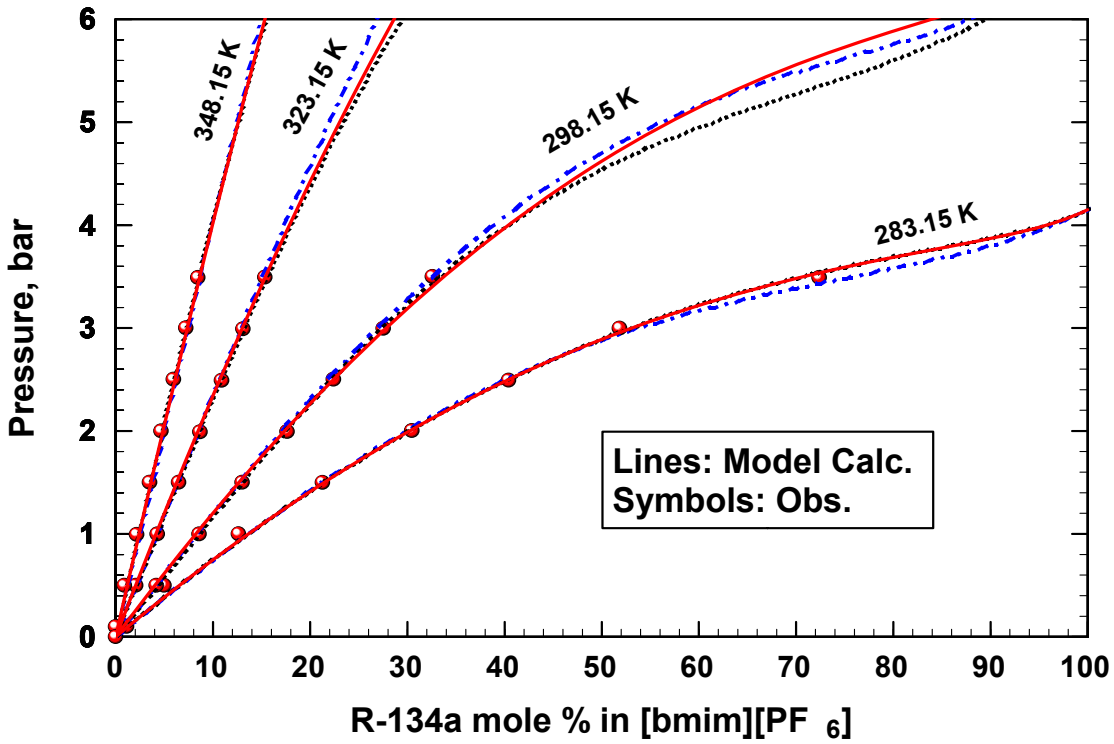

Figure 2. Isothermal *Px* (solubility) diagram for R-134a / [bmim][PF_6] mixtures. Solid lines: Wilson activity model; Dotted lines: NRTL model; Broken lines: Margules model; Symbols: the present experimental data.

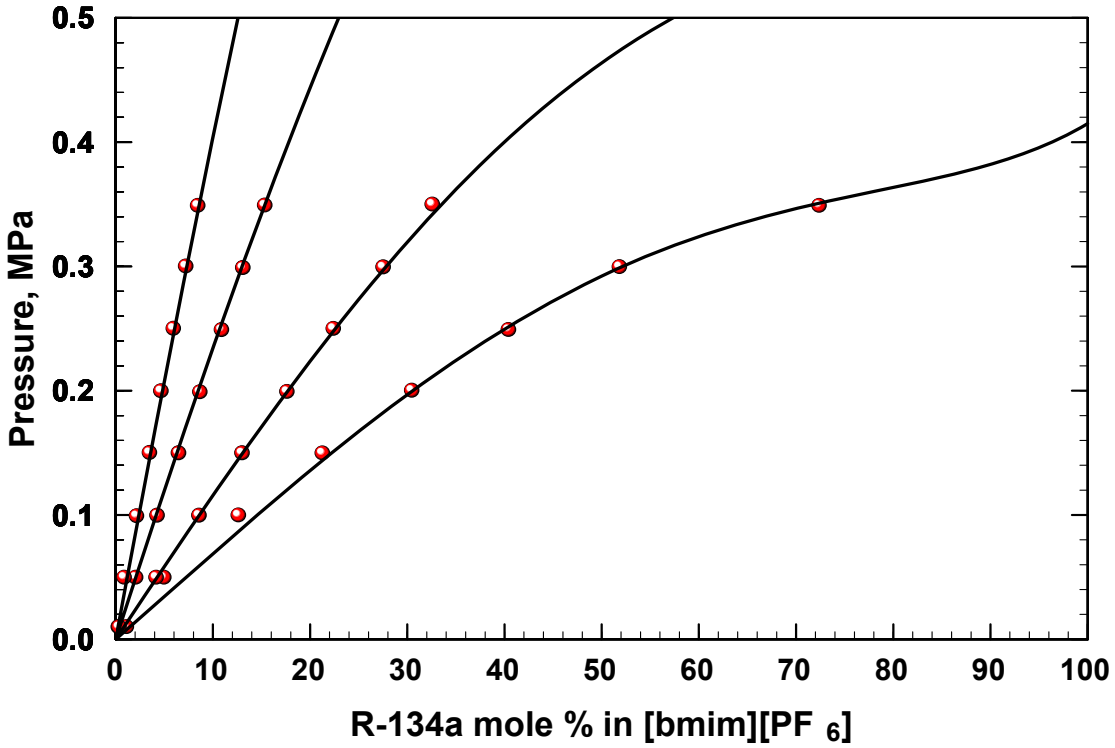

Figure 3. Isothermal *Px* (solubility) diagram for R-134a / [bmim][PF_6]. Lines: NRTL model calculations; Symbols: the present experimental data.

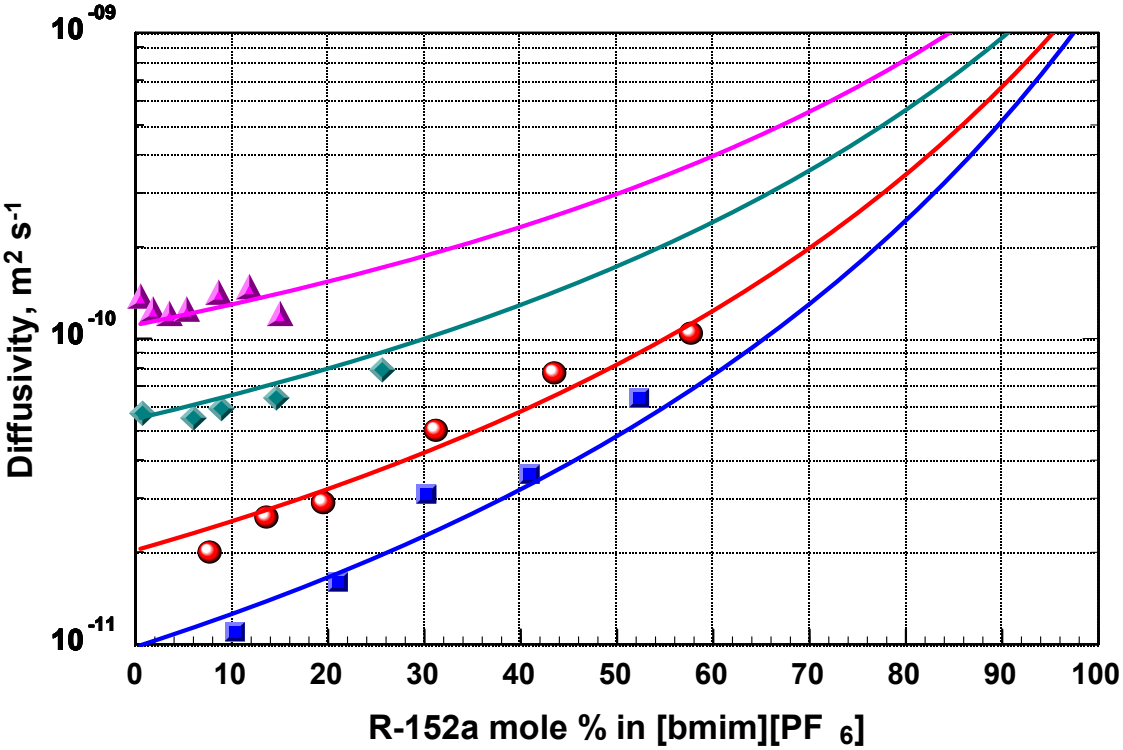

Figure 4. Diffusivity *versus* composition diagram of R-152a in [bmim][PF_6]: Lines: model calculations (see Text); Symbols: the present experimental data.

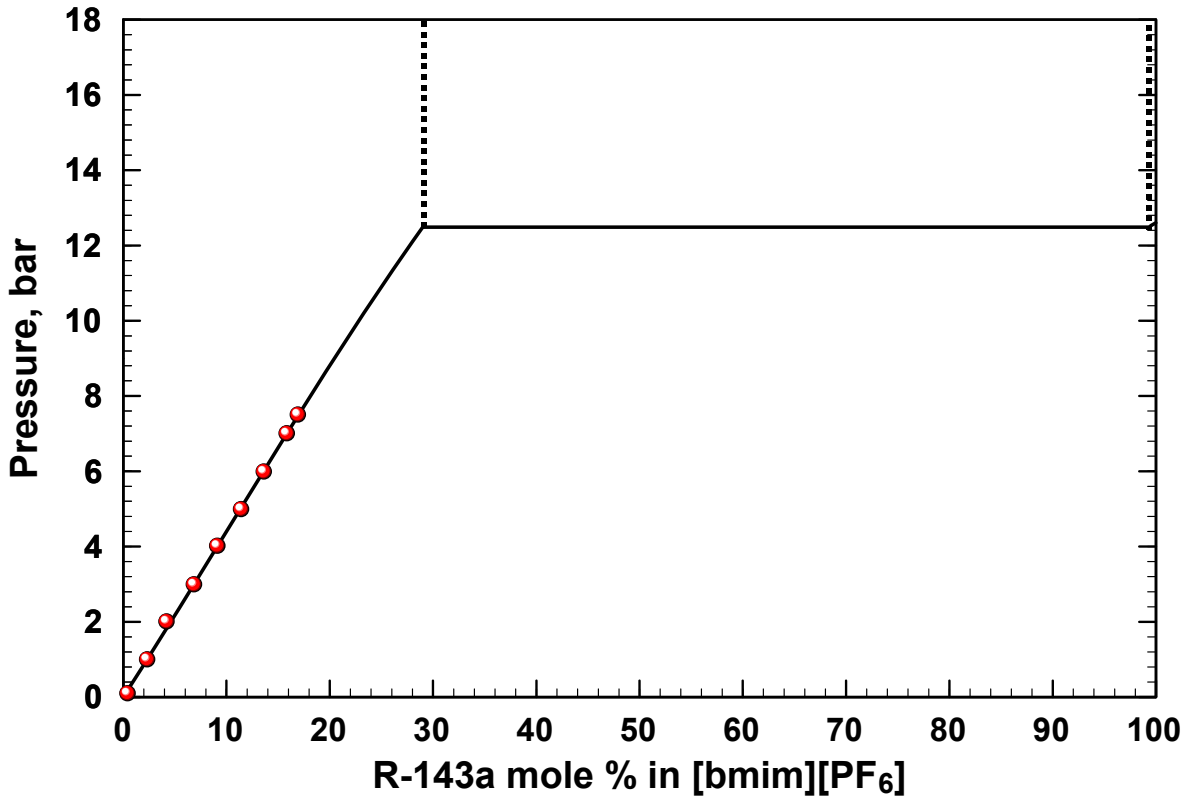

Figure 5. Predictions of phase behaviors for R-143a in [bmim][PF_6] with present NRTL model at 298.2 K.